



Modal propagation and interaction in the smooth transition from a metal mushroom structure to a bed-of-nails-type wire medium

Alexander B. Yakovlev and George W. Hanson

Citation: *J. Appl. Phys.* **111**, 074308 (2012); doi: 10.1063/1.3699036

View online: <http://dx.doi.org/10.1063/1.3699036>

View Table of Contents: <http://jap.aip.org/resource/1/JAPIAU/v111/i7>

Published by the [American Institute of Physics](#).

Related Articles

Modulation of electromagnetic waves by alternating currents through left-handed ferromagnetic microwires
J. Appl. Phys. **111**, 063901 (2012)

Reflection characteristics of a composite planar AMC surface
AIP Advances **2**, 012128 (2012)

Broadband polarization transformation via enhanced asymmetric transmission through arrays of twisted complementary split-ring resonators
Appl. Phys. Lett. **99**, 221907 (2011)

Broad band invisibility cloak made of normal dielectric multilayer
Appl. Phys. Lett. **99**, 154104 (2011)

Multi-beam generations at pre-designed directions based on anisotropic zero-index metamaterials
Appl. Phys. Lett. **99**, 131913 (2011)

Additional information on *J. Appl. Phys.*

Journal Homepage: <http://jap.aip.org/>

Journal Information: http://jap.aip.org/about/about_the_journal

Top downloads: http://jap.aip.org/features/most_downloaded

Information for Authors: <http://jap.aip.org/authors>

ADVERTISEMENT



FIND THE NEEDLE IN THE HIRING HAYSTACK

Post jobs and reach
thousands of hard-to-find
scientists with specific skills



<http://careers.physicstoday.org/post.cfm>

physicstoday JOBS

Modal propagation and interaction in the smooth transition from a metal mushroom structure to a bed-of-nails-type wire medium

Alexander B. Yakovlev¹ and George W. Hanson²

¹*Department of Electrical Engineering, The University of Mississippi, University, Mississippi 38677, USA*

²*Department of Electrical Engineering, University of Wisconsin-Milwaukee, 3200 N. Cramer St., Milwaukee, Wisconsin 53211, USA*

(Received 19 November 2011; accepted 27 February 2012; published online 5 April 2012)

Natural propagation modes of a metamaterial mushroom structure are studied as the patch material transitions from being a perfect conductor to being transparent, in which case the structure becomes a bed-of-nails medium. It is shown that the modes of the perfectly conducting structure smoothly continue to those of the bed-of-nails structure in the complex wavenumber plane, except for some modal interaction regions and degeneracy points associated with complex-frequency branch points migrating across the real frequency axis. © 2012 American Institute of Physics. [<http://dx.doi.org/10.1063/1.3699036>]

I. INTRODUCTION

Artificial electromagnetic materials such as mushroom and bed-of-nails structures can exhibit interesting anomalous phenomena, such as negative refraction¹ and sub-wavelength imaging,² and they also have applications as electrically thin absorbers³ and high-impedance surfaces for low-profile antenna applications.^{4,5} As is now well known, wire media (e.g., bed-of-nails) exhibit strong spatial dispersion at microwave frequencies,⁶ such that nonlocal homogenization methods with additional boundary conditions (ABCs) are essential in analyzing these structures.^{7–10} It is also known that mushroom structures composed of metallic patches¹¹ suppress or significantly reduce spatial dispersion in wire media.^{12–15} The presence of metallic patches at the wire ends diminishes charge buildup in such a way that upon homogenization, the mushroom structure can be treated as a uniaxial continuous epsilon-negative local material loaded with a capacitive grid of patches. However, when the patches are thin resistive materials, such as extremely thin metals or graphene, charge accumulation and diffusion at the wire-to-patch interface becomes important and spatial dispersion effects have to be considered, necessitating an additional boundary condition at this interface.¹⁶ Upon homogenization, these charge effects are reflected in the nonlocal slab permittivity.

In general, in a mushroom structure the patches can vary from perfect electrical conductors (PECs) to transparent (bed-of-nails medium). This can be examined in a unified model if one considers the patch as a two-dimensional material represented by a surface conductivity σ_{2d} (S). The limit $\sigma_{2d} \rightarrow \infty$ represents the PEC case, and $\sigma_{2d} \rightarrow 0$ represents the transparent case. Moreover, graphene or other extremely thin materials exhibit complex-valued Drude surface conductivities, typically in the mS range¹⁷ (for graphene at low GHz frequencies, the real part of σ_{2d} is much larger than the imaginary part), and are of interest because in the case of graphene, σ_{2d} is tunable by means of electrostatic or magnetostatic bias. In this work, we consider a mushroom structure with a general patch conductivity σ_{2d} and examine the

natural propagation modes of the structure as the patch conductivity varies between the two limits $\sigma_{2d} \rightarrow \infty$ and $\sigma_{2d} \rightarrow 0$. It is shown that the modes of the PEC patch structure smoothly continue to those of the bed-of-nails structure in the complex wavenumber plane, except for some modal interaction regions and degeneracy points associated with complex-frequency branch points migrating across the real frequency axis. Physically important leaky modes in each limit become complex modes for intervening values of σ_{2d} . An understanding of these propagating modes is important for structures having patches consisting of thin metals or graphene. The modal spatial dependence in the propagation direction is $e^{-jk_z z}$, such that physical proper complex poles are located in the first and third quadrants of the k_z -plane and physical improper complex poles are in the second and fourth quadrants of the k_z -plane. In this regard, the proper solutions (complex or real above cutoff) are defined on the proper Riemann sheet of the k_z -plane, with the field decaying in the air region in the vertical direction away from the patch interface, and the improper solutions (complex or real below cutoff) are defined on the improper Riemann sheet of the k_z -plane, with the field growing in the vertical direction. Physical and non-physical complex solutions are determined by their behavior at infinity in the propagating direction along the interface and by the fast or slow regimes of operation, respectively. However, a rigorous definition of physical and non-physical complex solutions comes from an excitation problem (in the sense that physical complex poles contribute to the radiation field). Further details on modal terminology and a description of leaky waves can be found in Refs. 18–22. Throughout this paper, we use the International system of units, and the (suppressed) time dependence is $e^{j\omega t}$.

II. NONLOCAL HOMOGENIZATION MODEL FOR MUSHROOM SURFACES WITH THIN METAL/ GRAPHENE PATCHES

Figure 1 depicts a mushroom medium in which the patches are assumed to be a thin imperfectly conducting material. With $k_0\sqrt{\epsilon_r}a \ll \pi$ and $a/L > 1$, in which k_0 is the

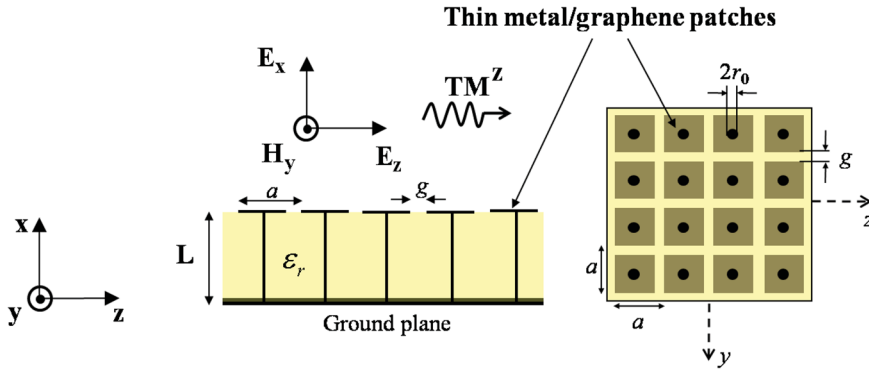


FIG. 1. Wire medium consisting of mushroom surfaces with thin material patches.

free-space wavenumber, L is the thickness of the slab, and a is the period of the two-dimensional lattice of square patches (a is the wire period if the patches are absent), the wire medium can be replaced with a homogenized, spatially dispersive uniaxial material slab having a thickness L and tensor permittivity $\underline{\epsilon}(\mathbf{q}, \omega)$, where $\mathbf{q} = \hat{x}q$ is a vertical wavenumber.^{6,13,16,23} The presence of spatial dispersion necessitates an additional boundary condition at each material interface (i.e., at each wire termination).

Although the structure will support both transverse-magnetic (TM^z , having E_x, E_z , and H_y field components) and transverse-electric (TE^z , having H_x, H_z , and E_y field components) modes, we restrict our attention to TM^z modes, because TE^z modes will not interact with the wires, and the resulting homogenized slab is local. In what follows, the term “microscopic” refers to currents and fields in the microstructure of the medium, i.e., on the wires and patches of the actual physical structure. The term “macroscopic” refers to averaged (homogenized) fields, i.e., the fields in the equivalent homogenized medium.

In Ref. 16, an ABC was presented for the termination of a wire at an imperfect conductor sufficiently thin so that the field penetrates through the material. The material is modeled by a two-dimensional complex surface conductivity σ_{2d} (S). This model is appropriate for two-dimensional materials such as graphene or for sufficiently thin three-dimensional materials. In the latter case, $\sigma_{2d} = \sigma_{3d}t$, in which σ_{3d} (S/m) is the usual complex conductivity and $t \ll \delta$ is the material thickness, with $\delta = \sqrt{2/\omega\mu_0\sigma_{3d}}$ being the skin depth. On the two-dimensional material, which is assumed to be local and isotropic, the microscopic current and field are related as $J_s(x, z) = \sigma_{2d}E_s(x, z)$, where J_s is the surface current density (A/m) and E_s is the tangential electric field. The current density on the wire is $J_c(x)$, and enforcing the continuity of current between the wire and patch, $J_c(x_0) = J_s$, results in the generalized ABC (GABC) (Ref. 16)

$$J_c(x_0) + \frac{\sigma_{2d}}{j\omega\epsilon_0\epsilon_r} \frac{dJ_c(x)}{dx} \Big|_{x_0} = 0. \quad (1)$$

In terms of macroscopic fields,

$$\left(1 + \frac{\sigma_{2d}}{j\omega\epsilon_0\epsilon_r} \frac{d}{dx}\right) (k_0\epsilon_r E_x - k_z\eta_0 H_y) \Big|_{x_0} = 0, \quad (2)$$

in which k_z is the propagation constant. If $\sigma_{2d} \rightarrow 0$, the boundary condition recovers the case of an open-ended wire (not terminated by a ground plane or patch),⁸

$$J_c(x_0) = 0, \quad (3)$$

and if $\sigma_{2d} \rightarrow \infty$, the ABC for termination in a perfect conductor is obtained.^{8,13,14}

$$\frac{dJ_c(x)}{dx} \Big|_{x_0} = 0. \quad (4)$$

Upon homogenization, the material slab has tensor permittivity,²³

$$\underline{\epsilon}_{\text{eff}}(q) = \epsilon_0\epsilon_r(\epsilon_{xx}(q)\hat{x}\hat{x} + \hat{y}\hat{y} + \hat{z}\hat{z}), \quad (5)$$

in which $\epsilon_{xx}(q) = 1 - \beta_p^2/(k^2 - q^2)$, $k = k_0\sqrt{\epsilon_r}$, and $\beta_p^2 = (2\pi/a^2)/(\ln(a/2\pi r_0) + 0.5275)$, with β_p being the plasma wavenumber. The TM^z plane wave incidence problem is solved in Ref. 16, and here we obtain the dispersion equation for natural modes. Assuming that the material patches are replaced by a continuous surface impedance Z_g , we enforce the macroscopic two-sided (or sheet) impedance boundary condition $E_z(x=L^-) = E_z(x=L^+) = -Z_g(H_y(x=L^+) - H_y(x=L^-))$. The GABC (2) is enforced at $x=L^-$, and, assuming a PEC ground plane, (2) in the limit $\sigma_{2d} \rightarrow \infty$ is enforced at $x=0$. The grid impedance Z_g is provided as^{16,24,25}

$$Z_g = \frac{a}{(a-g)\sigma_{2d}} - j\frac{\eta_{\text{eff}}}{2\alpha}, \quad (6)$$

where $\alpha = (k_{\text{eff}}a/\pi)\ln(\csc(\pi g/2a))$, $\eta_{\text{eff}} = \eta_0/\sqrt{\epsilon_{\text{eff}}}$, $k_{\text{eff}} = k_0\sqrt{\epsilon_{\text{eff}}}$, $\epsilon_{\text{eff}} = (\epsilon_r + 1)/2$, and $\eta_0 = \sqrt{\mu_0/\epsilon_0}$. The resulting dispersion equation is

$$Z(k_z) = K \coth(\gamma_{\text{TM}}L) \cot(kL) + \left(\frac{1}{\gamma_0} - j\frac{\eta_0}{Z_g k_0}\right) = 0, \quad (7)$$

where $K = N/D$,

$$N = \left(\frac{1}{\epsilon_{xx}^{\text{TM}}} - 1\right) \left(\frac{\sigma_{2d}\gamma_{\text{TM}} \tanh(\gamma_{\text{TM}}L) + 1}{j\omega\epsilon_0\epsilon_r}\right) + \left(1 - \frac{\sigma_{2d}k}{j\omega\epsilon_0\epsilon_r} \tan(kL)\right), \quad (8)$$

$$D = -\frac{k}{\epsilon_r} \left(\frac{1}{\epsilon_{xx}^{\text{TM}}} - 1\right) \left(\frac{\sigma_{2d}\gamma_{\text{TM}}}{j\omega\epsilon_0\epsilon_r} + \coth(\gamma_{\text{TM}}L)\right) + \frac{\gamma_{\text{TM}}}{\epsilon_r} \left(\cot(kL) - \frac{\sigma_{2d}k}{j\omega\epsilon_0\epsilon_r}\right), \quad (9)$$

$\gamma_0^2 = k_z^2 - k_0^2$, $\gamma_{\text{TM}}^2 = \beta_p^2 + k_z^2 - k^2$, and $\epsilon_{xx}^{\text{TM}} = 1 - \beta_p^2 / (k_z^2 + \beta_p^2)$. In the limiting case of $\sigma_{2d} \rightarrow 0$, we have the wire medium (bed-of-nails) result,²³ and for $\sigma_{2d} \rightarrow \infty$ we have the PEC patch result.^{13,14} In both limits $\sigma_{2d} \rightarrow 0$ and ∞ , the GABC and transmission/reflection problems have been verified^{14,16} using HFSS.²⁶

III. RESULTS

The results presented in this section are based on the numerical solution of the dispersion equation (7) as a root search for the propagation constant k_z of the natural waves of the structure, which in general include real and complex and proper and improper solutions. The purpose of this study is two-fold. First, we analyze the propagation properties of bound and leaky waves during the transition of a mushroom structure with PEC patches to a bed-of-nails wire-medium slab, i.e., as σ_{2d} varies from infinity to zero. The transition and resulting modal behavior shed light on the role of patch conductivity in mode propagation. Second, we demonstrate that for some values of surface conductivity, mode interaction results in mode transformation, and this occurs for very small variations in the value of the surface conductivity.

We begin with the known case of a mushroom structure with PEC patches studied in Ref. 14. The dispersion behavior of the modal spectrum is demonstrated in Fig. 2 (see Fig. 19 in Ref. 14, obtained for the same structural parameters, in which a detailed description of modal behavior is provided), which serves as a starting point for the analysis to follow. Note that the structure is lossless, and so proper and improper real modes and complex leaky modes exist. Here, we briefly summarize the dispersion behavior for different modes. In Fig. 2, at low frequencies there is a highly dispersive surface wave (proper real bound mode) that propagates in the backward direction due to the negative slope of the dispersion curve. At approximately 9.1 GHz, modal propagation stops (corresponding to the left-hand edge of the stop band region for surface waves), and the mode becomes a proper complex (leaky wave) solution that enters a fast-wave region at approximately 10 GHz ($0 < \text{Re}(k_z/k_0) < 1$), wherein it radiates in the sense of leaky-wave radiation in the backward direction in the spatial quadrant with $x > 0$, $z > 0$. At a plasma frequency of 12.14 GHz, the pole of the proper complex solution crosses the Sommerfeld branch cut in the complex k_z -plane and becomes an improper complex (leaky wave) mode radiating in the forward direction in the spatial quadrant $x > 0$, $z < 0$ within the fast-wave region ($-1 < \text{Re}(k_z/k_0) < 0$). With an increase in frequency it eventually becomes one of the improper real solutions. Also, at low frequencies there is another surface wave (proper real bound mode) propagating in the forward direction with very low dispersion, which becomes a nonphysical proper complex solution at the leaky-wave cutoff of 9.1 GHz. This nonphysical solution is not of practical interest in the lossless case (even though it continues to a physical surface-wave higher-order mode at higher frequencies, as explained in Ref. 14); however, it becomes important in the lossy case, as is shown below. In addition, in Fig. 2 the second forward sur-

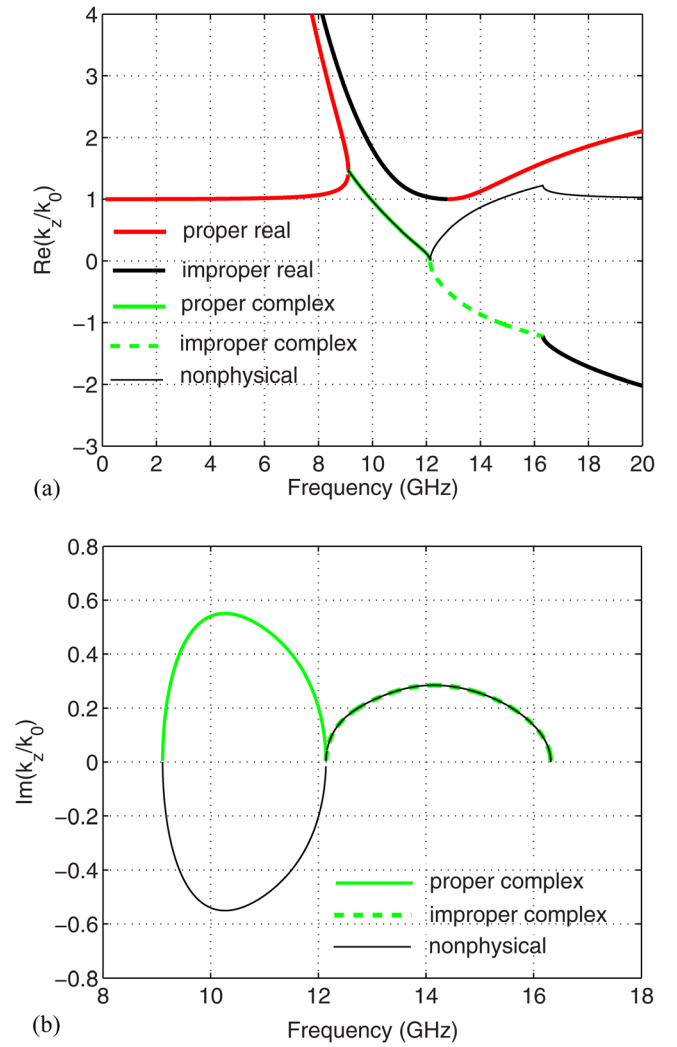


FIG. 2. Dispersion behavior ((a) phase constant and (b) attenuation constant) of the natural modes of the mushroom structure with PEC patches. Parameters of the structure: $a = 2$ mm, $g = 0.2$ mm, $L = 1$ mm, $r_0 = 0.05$ mm, and $\epsilon_r = 10.2$.

face wave is shown, with a cutoff frequency at 12.7 GHz, which continues as an improper real solution at lower frequencies.

With this understanding of the modal spectrum of the structure with PEC patches, we proceed with the analysis of modal propagation as the mushroom structure is converted to a wire-medium slab via a gradual reduction of the surface conductivity of the thin patch material. In all the figures to follow, proper complex solutions are denoted with solid lines, and improper complex solutions with dashed lines. We first analyze the physical branch consisting of analytically continued proper real (backward), proper complex, and improper complex solutions shown in Fig. 2, which become perturbed complex solutions in the presence of conduction losses (e.g., the proper real bound modes (red curves in Fig. 2) become complex modes in the presence of loss).

In Fig. 3, results are shown for a range of surface conductivities σ_{2d} . At the largest value, $\sigma_{2d} = 5.8$ S, this physical branch is only slightly perturbed from that described for the PEC case (compare with Fig. 2). If we assume a bulk

conductivity of $\sigma_{3d} = 5.8 \times 10^7$ S/m, the associated metal thickness for $\sigma_{2d} = 5.8$ S is $t = 100$ nm, well below the skin depth, which is in the micron range. This means that typical conduction losses due to skin depth do not affect the modal behavior even by significantly reducing the metal thickness to 100 nm.

As the surface conductivity is further reduced, it is observed that the complex waves become significantly perturbed and attenuate very rapidly due to the large values of the attenuation constant (shown in Fig. 3(b)). An interesting observation is that if the surface conductivity is decreased to the point at which the patches become almost transparent ($\sigma_{2d} = 5.8 \times 10^{-6}$ S), these complex waves turn into physical leaky waves of the wire-medium slab above 23.5 GHz, specifically, a physical proper complex mode which continues as a physical improper complex mode at a frequency of 26.4 GHz (compare with Fig. 11 in Ref. 14 for the case of a 2 mm period). This demonstrates that the physical leaky waves (proper complex and improper complex) of the mushroom structure with PEC patches smoothly transition to perturbed complex waves (due to the presence of conduction losses), which eventually become physical leaky waves (proper com-

plex and improper complex) of the wire-medium slab as the surface conductivity of the patches is suitably decreased.

Next, we consider the modal dynamics of proper real (surface waves) and improper real solutions, including the nonphysical branch shown in Fig. 2. If we start with the PEC case and gradually reduce the surface conductivity, the proper and improper real solutions become significantly perturbed. However, what is interesting is that at some value of surface conductivity, the modal behavior dramatically changes. In Fig. 4, it is shown that the modal behavior is very different for two values of surface conductivity, $\sigma_{2d} = 0.058$ S and $\sigma_{2d} = 0.116$ S (see the frequency range from 12 GHz to 14 GHz, wherein the modal curves interchange behavior). This leads to the conclusion that in between these values of surface conductivity there is a value at which modal degeneracy occurs.

With smooth variation of the surface conductivity between the values of 0.058 S and 0.116 S, a detailed analysis of the modal behavior shown in Fig. 4 reveals modal interchange occurring at approximately $\sigma_{2d} = 0.06257$ S. In order to understand and explain the mechanism of modal interaction (in the sense of modal transformation), we refer

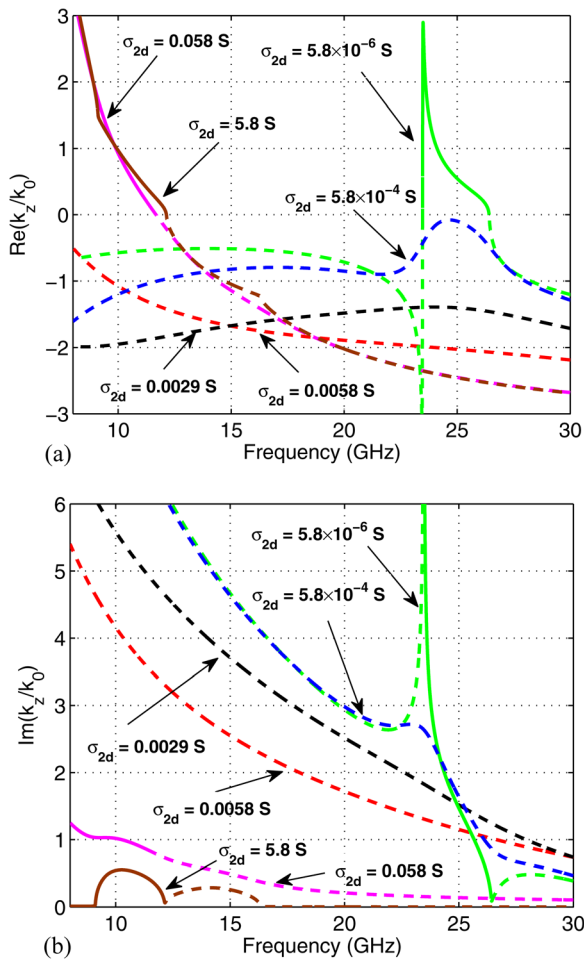


FIG. 3. Modal propagation ((a) phase constant and (b) attenuation constant) of proper complex and improper complex modes as the mushroom structure is transformed to a wire-medium slab with decreasing surface conductivity of the material patches. It is observed that the physical leaky waves of the mushroom structure smoothly transition to the physical leaky waves of the wire-medium slab.

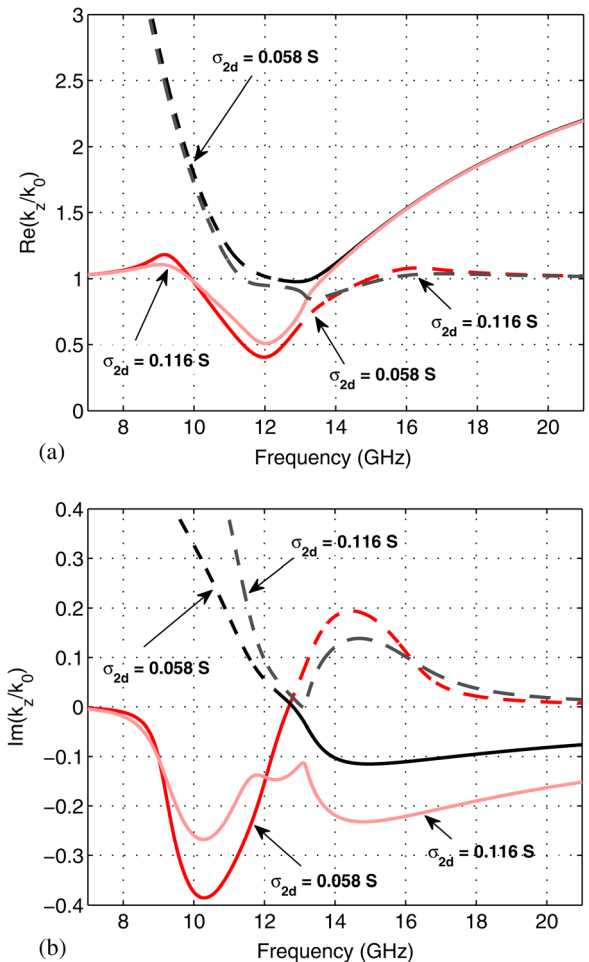


FIG. 4. Modal dynamics ((a) phase constant and (b) attenuation constant) of complex waves for two values of the surface conductivity (0.058 S and 0.116 S) showing qualitatively different behavior.

to our previous works on the analysis of similar phenomena that occur in traditional guided-wave structures.^{27–30} In those papers and references therein, we developed a mathematical framework that concerns the dynamics of frequency-plane branch-point singularities of the dispersion function, which separate different branches of solutions (positive and negative, complex and complex-conjugate, and n and $n + 2$ TM (TE) modes), such that a complete rotation about branch points in the complex frequency plane results in the smooth interchange of solutions. Using the terminology given in Refs. 27–30, we are particularly interested in the type 2 branch points, $\omega_{n,n+2}^{(2)}$, which connect n and $n + 2$ different modes within a given class (TM or TE). These complex frequency-plane branch points are obtained as numerical solutions of the system of nonlinear equations

$$Z(k_z, \omega) = Z'_{k_z}(k_z, \omega) = 0, \quad (10)$$

$$Z'_{\omega}(k_z, \omega)Z''_{k_z k_z}(k_z, \omega) \neq 0, \quad (11)$$

where $Z(k_z, \omega)$ is the dispersion function given by (7) and prime and double-prime symbols denote the first and second derivatives of the dispersion function with respect to the subscripted quantity. For a given example of a mushroom structure with thin material patches, the complex frequency-plane branch points $\omega_{n,n+2}^{(2)}$ have been calculated for different values of the surface conductivity. Figure 5 shows the evolution of the branch points in the complex frequency plane as a function of surface conductivity. As discussed in Refs. 27–30, when the branch point is below and near the real frequency axis in the complex frequency plane, modal interaction occurs, and the modal behavior is significantly perturbed. With further reduction of the value of the surface conductivity, the branch point approaches the real frequency axis, and at the value of $\sigma_{2d} = 0.06257$ S it crosses the real frequency axis, at which point the modal degeneracy occurs. As we further decrease the value of the surface conductivity, the branch point is near and above the real frequency axis

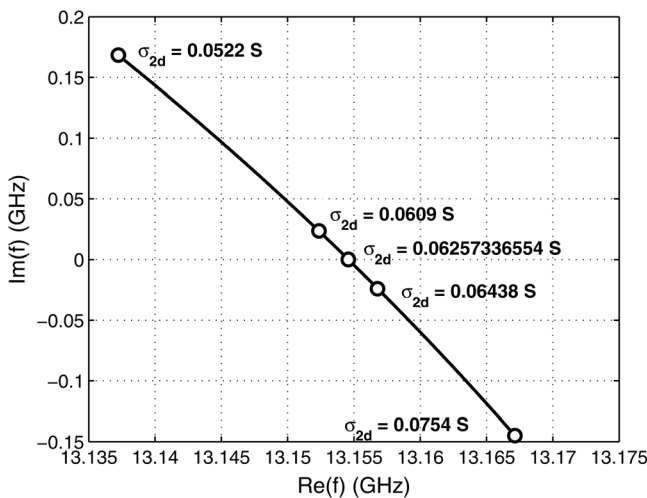


FIG. 5. Evolution of a complex frequency-plane branch point parameterized by surface conductivity. The branch point controls the modal interaction, and the positions of the branch point (below, above, or on the real frequency axis) correspond to different modal behaviors.

(e.g., for $\sigma_{2d} = 0.0609$ S as shown in Fig. 5). This migration through the real-frequency axis corresponds to the modal interchange (modal transformation) in the pair of solutions.

In order to demonstrate that the modal interaction occurs due to the presence of complex frequency-plane branch points, in Fig. 6 we present the results for the pair of complex solutions obtained at the values of surface conductivity considered in Fig. 5. It is observed that the modal degeneracy occurs at $\sigma_{2d} = 0.06257$ S, at which point the branch point crosses the real frequency axis. Also, it can be seen that the modal behavior for the values of $\sigma_{2d} = 0.06438$ S and $\sigma_{2d} = 0.0609$ S is qualitatively very different, demonstrating the modal interchange associated with branch points located below and above the real frequency axis in the complex frequency plane. Also, it should be noted that for the specific example considered here, we observed a second modal interaction region with a degeneracy point, which occurs at the surface conductivity $\sigma_{2d} = 0.0389$ S (the results are not shown here for the sake of brevity).

To complete the analysis of the modal propagation of surface (bound) waves in the transition from PEC patches to a wire-medium slab, we further reduce the surface conductivity

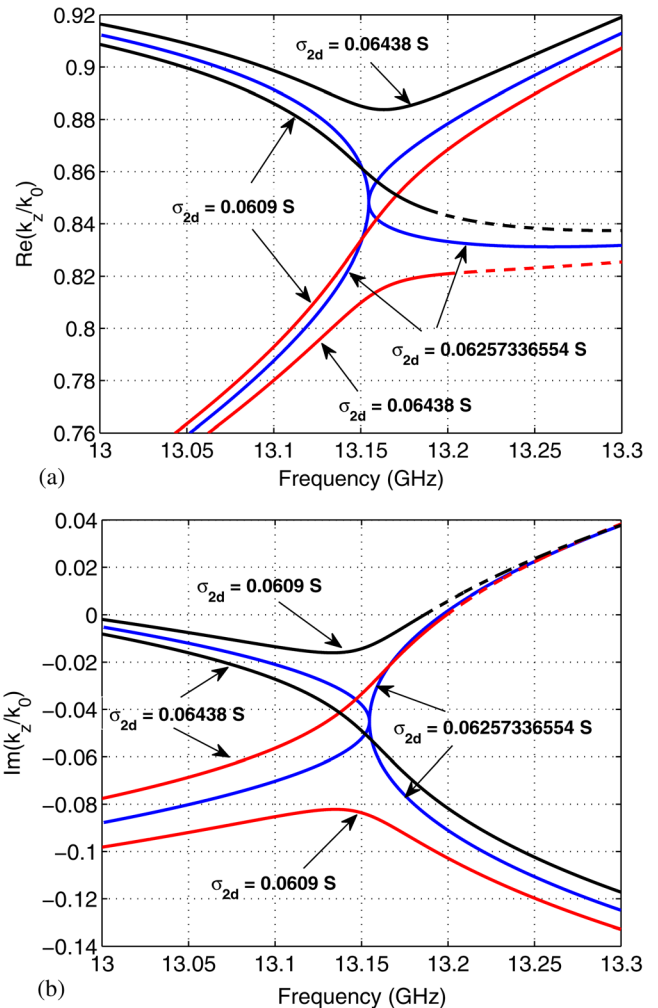


FIG. 6. Modal interaction and modal degeneracy ((a) phase constant and (b) attenuation constant) for the pair of complex solutions due to the presence of complex frequency-plane branch points.

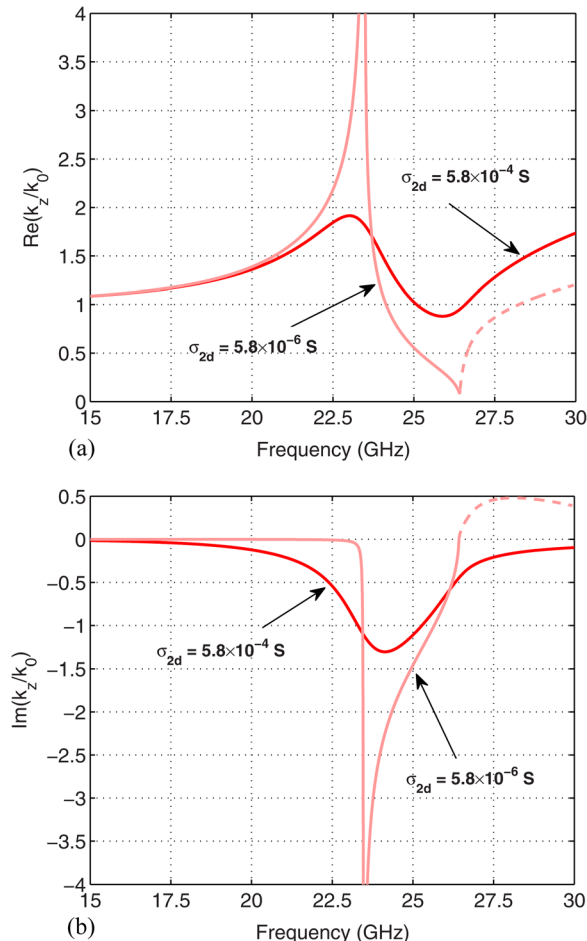


FIG. 7. Modal propagation (a) phase constant and (b) attenuation constant of the perturbed surface-wave mode of the mushroom structure in the transition to the wire-medium slab.

and consider the very small values shown in Fig. 7. It can be seen that the perturbed forward surface-wave mode (which becomes a complex solution) of the mushroom structure with almost transparent patches ($\sigma_{2d} = 5.8 \times 10^{-6}$ S) becomes the surface-wave mode of the wire-medium slab with the characteristic stop band behavior observed in wire media (the results are in excellent agreement with those shown for the wire-medium slab in Fig. 7 of Ref. 14). It is observed that at higher frequencies, the surface wave of the wire-medium slab continues as a nonphysical proper complex solution that becomes a nonphysical improper complex solution (see Fig. 3 in this paper and Fig. 11 in Ref. 14 in the frequency range above 23.5 GHz, wherein physical proper complex and physical improper complex solutions are shown).

IV. CONCLUSIONS

Natural propagation modes of a metamaterial mushroom structure consisting of material patches having a two-dimensional surface conductivity σ_{2d} have been studied as the patch material transitions from a perfect conductor to transparent, in which case the structure becomes a bed-of-nails medium. It is shown that the propagation modes of the perfectly conducting structure smoothly continue to those of the bed-of-nails structure in the complex wavenumber plane,

except for some modal interaction regions and degeneracy points associated with complex-frequency branch points migrating across the real axis.

- ¹V. G. Veselago, "The electrodynamics of substances with simultaneously negative values of ϵ and μ ," *Sov. Phys. Usp.* **10**, 509–514 (1968).
- ²J. B. Pendry, "Negative refraction makes a perfect lens," *Phys. Rev. Lett.* **85**, 03966 (2000).
- ³O. Luukkonen, F. Costa, C. Simovski, A. Monorchio, and S. Tretyakov, "A thin electromagnetic absorber for wide incidence angles and both polarizations," *IEEE Trans. Antennas Propag.* **57**, 3119–3125 (2009).
- ⁴F. Yang and Y. Rahmat-Samii, "Reflection phase characterization of the EBG ground plane for low profile wire antenna applications," *IEEE Trans. Antennas Propag.* **51**, 2691–2703 (2003).
- ⁵A. P. Feresidis, G. Goussetis, S. Wang, and J. C. Vardaxoglou, "Artificial magnetic conductor surfaces and their application to low-profile high-gain planar antennas," *IEEE Trans. Antennas Propag.* **53**, 209–215 (2005).
- ⁶P. A. Belov, R. Marqués, S. I. Maslovski, I. S. Nefedov, M. Silveirinha, C. R. Simovski, and S. A. Tretyakov, "Strong spatial dispersion in wire media in the very large wavelength limit," *Phys. Rev. B* **67**, 113103 (2003).
- ⁷M. G. Silveirinha, C. A. Fernandes, and J. R. Costa, "Electromagnetic characterization of textured surfaces formed by metallic pins," *IEEE Trans. Antennas Propag.* **56**(2), 405–415 (2008).
- ⁸M. G. Silveirinha, C. A. Fernandes, and J. R. Costa, "Additional boundary condition for a wire medium connected to a metallic surface," *New J. Phys.* **10**, 053011 (2008).
- ⁹M. G. Silveirinha, "Additional boundary condition for the wire medium," *IEEE Trans. Antennas Propag.* **54**, 1766–1780 (2006).
- ¹⁰S. I. Maslovski, T. A. Morgado, M. G. Silveirinha, C. S. R. Kaipa, and A. B. Yakovlev, "Generalized additional boundary conditions for wire media," *New J. Phys.* **12**, 113047 (2010).
- ¹¹D. Sievenpiper, L. Zhang, R. Broas, N. Alexopoulos, and E. Yablonovitch, "High-impedance electromagnetic surfaces with a forbidden frequency band," *IEEE Trans. Microwave Theory Tech.* **47**, 2059–2074 (1999).
- ¹²A. Demetriadou and J. Pendry, "Taming spatial dispersion in wire metamaterial," *J. Phys.: Condens. Matter* **20**, 295222 (2008).
- ¹³O. Luukkonen, M. Silveirinha, A. Yakovlev, C. Simovski, I. Nefedov, and S. Tretyakov, "Effects of spatial dispersion on reflection from mushroom-type artificial impedance surfaces," *IEEE Trans. Microwave Theory Tech.* **57**, 2692–2699 (2009).
- ¹⁴A. Yakovlev, M. Silveirinha, O. Luukkonen, C. Simovski, I. Nefedov, and S. Tretyakov, "Characterization of surface-wave and leaky-wave propagation on wire-medium slabs and mushroom structures based on local and nonlocal homogenization models," *IEEE Trans. Microwave Theory Tech.* **57**, 2700–2714 (2009).
- ¹⁵C. S. R. Kaipa, A. B. Yakovlev, and M. G. Silveirinha, "Characterization of negative refraction with multilayered mushroom-type metamaterials at microwaves," *J. Appl. Phys.* **109**, 044901 (2011).
- ¹⁶A. B. Yakovlev, Y. R. Padooru, G. W. Hanson, A. Mafi, and S. Karbasi, "A generalized additional boundary condition for mushroom-type and bed-of-nails-type wire media," *IEEE Trans. Microwave Theory Tech.* **59**, 527–532 (2011).
- ¹⁷G. Hanson, "Dyadic Green's functions and guided surface waves on graphene," *J. Appl. Phys.* **103**, 064302 (2008).
- ¹⁸T. Tamir and A. A. Oliner, "Guided complex waves, Part I: Fields at an interface," *Proc. Inst. Electr. Eng.* **110**, 310–324 (1963).
- ¹⁹T. Tamir and A. A. Oliner, "Guided complex waves, Part II: Relation to radiation patterns," *Proc. Inst. Electr. Eng.* **110**, 325–334 (1963).
- ²⁰T. Tamir and A. A. Oliner, "The spectrum of electromagnetic waves guided by a plasma layer," *Proc. IEEE* **51**, 317–332 (1963).
- ²¹A. Hessel, "General characteristics of traveling wave antennas," in *Antenna Theory*, edited by R. E. Collin and F. J. Zucker (McGraw-Hill, New York, 1969), pp. 151–258.
- ²²A. A. Oliner and D. R. Jackson, "Leaky-wave antennas," in *Modern Antenna Handbook*, edited by J. L. Volakis (McGraw-Hill, New York, 2007), pp. 11-1–11-56.
- ²³M. Silveirinha, C. Fernandes, and J. Costa, "Electromagnetic characterization of textured surfaces formed by metallic pins," *IEEE Trans. Antennas Propag.* **56**, 405–415 (2008).
- ²⁴S. Tretyakov, *Analytical Modeling in Applied Electromagnetics* (Artech House, 2003).

- ²⁵O. Luukkonen, C. Simovski, G. Grant, G. Goussetis, D. Lioubtchenko, A. Raisanen, and S. Tretyakov, "Simple and accurate analytical model of planar grids and high-impedance surfaces comprising metal strips and patches," *IEEE Trans. Antennas Propag.* **56**, 1624–1632 (2008).
- ²⁶HFSS: High Frequency Structure Simulator based on Finite Element Method, Ansoft Corporation, <http://www.ansoft.com>.
- ²⁷G. W. Hanson and A. B. Yakovlev, "An analysis of leaky-wave dispersion phenomena in the vicinity of cutoff using complex frequency plane singularities," *Radio Sci.* **33**, 803–820 (1998).
- ²⁸G. W. Hanson and A. B. Yakovlev, "Investigation of mode interaction on planar dielectric waveguides with loss and gain," *Radio Sci.* **34**, 1349–1359 (1999).
- ²⁹A. B. Yakovlev and G. W. Hanson, "Mode transformation and mode continuation regimes on waveguiding structures," *IEEE Trans. Microwave Theory Tech.* **48**(1), 67–75 (2000).
- ³⁰A. B. Yakovlev and G. W. Hanson, "Fundamental modal phenomena on isotropic and anisotropic planar slab dielectric waveguides," *IEEE Trans. Antennas Propag.* **51**, 888–897 (2003).